

	SAKARYA ÜNİVERSİTESİ FEN BİLİMLERİ ENSTİTÜSÜ DERGİSİ <i>SAKARYA UNIVERSITY JOURNAL OF SCIENCE</i>		
	e-ISSN: 2147-835X Dergi sayfası: http://www.saujs.sakarya.edu.tr		
	<u>Received</u> 11-08-2017 <u>Accepted</u> 20-02-2018	<u>Doi</u> 10.16984/saufenbilder.334104	

Structural, Conformational and Spectroscopic Properties of C₁₆H₁₆BrNO₃ Schiff-Base Molecule: A Theoretical Investigation

Meryem Evecen*¹

ABSTRACT

Molecular geometry, vibrational frequencies and electronic properties (total energy, dipole moment, electronegativity, chemical hardness and softness) of the Schiff-bases compound C₁₆H₁₆BrNO₃ were investigated using DFT(B3LYP) method. Besides, the conformational analysis was made with respect to selected degrees of torsional freedom τ (C3C2C1N1) torsional. Molecular electrostatic potential, frontier molecular orbital energies and non linear optic analysis of molecule have been performed by using Gaussian 09W program. The non linear optic analysis indicates that this molecule can be evaluated as an attractive object for nonlinear optical material studies.

Keywords: Benzylidene, electronic properties, HOMO-LUMO, vibrational frequencies

1. INTRODUCTION

The Schiff-bases chemistry is very important due to their usage in anion sensors [1], thermochromism [2], photochromism [3], antifungal, antibacterial properties [4], antimicrobial activity [5], anticancer and antiinflammatory activities [6,7] and also in modern technologies. They may also both serve as reagents for stereo selective organic synthesis [8,9] and widely used as ligands in the formation of transition metal complexes[10]. In addition, they are used as non-linear optics compounds [11]. Therefore, a careful study of Schiff bases characteristics is important in their application successfully. Because of the structural characteristics of Schiff base products which contain electron donor and acceptor groups

connected through a conjugated chain, they will be the potential nonlinear optical (NLO) or electro-optical materials [12].

The important class of Schiff bases is benzylidene anilines. Generally, benzylidene anilines have been widely used in medicinal, biological chemistry and coordination and therefore their molecular and crystal structure have been of considerable interest by experimental and theoretical studies.

In [13], the IR spectra and X-ray crystallography of 4-bromo-*N*-(2,3,4-trimethoxybenzylidene) aniline (C₁₆H₁₆BrNO₃) was studied. In spite of widely usage of benzylidene anilines, the analysis of literature showed that no any computational study on BMBA molecule has been published yet. The objective of this study is to analyze the structural parameters, vibrational properties, frontier molecular orbital energies, conformational

* Corresponding Author

¹ Amasya University, Faculty of Arts and Sciences, Department of Physics, Amasya, e-mail: meryem.evecen@amasya.edu.tr

properties, natural atomic charges and NLO properties of the title molecule, 4-bromo-*N*-(2,3,4-trimethoxybenzylidene)aniline (BMBA), by density functional theory (DFT) technique in the B3LYP/6-311++G(d,p) level of theory and then compare our results with the available experimental work published before.

2. COMPUTATIONAL METHOD

For all the calculations on the BMBA, Gaussian 09 package was used [14] on the personal computer. Moreover, the X-ray coordinates in literature were utilised in order to obtain the initial guess of BMBA for modelling [13]. The structure optimization was done by density functional theory with the 6-311++G(d,p) basis set. The visual GaussView 5.0 [15] program was used in order to obtain the structural properties, electronic and vibrational spectra. The vibrational frequency signals were found real that confirm the optimized geometry and scaling factor of 0.96 was used for obtained frequencies [16].

3. RESULTS AND DISCUSSION

3.1. Geometry Optimization

The initial molecular geometry was directly taken from the X-ray diffraction experimental result without any constraints [13]. The crystal structure [13] and the theoretical geometric structure of BMBA molecule are shown in Fig. 1(a) and (b)-(e). BMBA's space group is $P\bar{1}$ and crystal structure is triclinic. These crystal structure parameters of the molecule are $a = 7.9103(3) \text{ \AA}$, $b = 9.9902(4) \text{ \AA}$, $c = 10.7821(3) \text{ \AA}$, $\alpha = 93.068(8)^\circ$, $\beta = 108.568(3)^\circ$, $\gamma = 109.679(3)^\circ$ and $V = 748.10(5) \text{ \AA}^3$ [13].

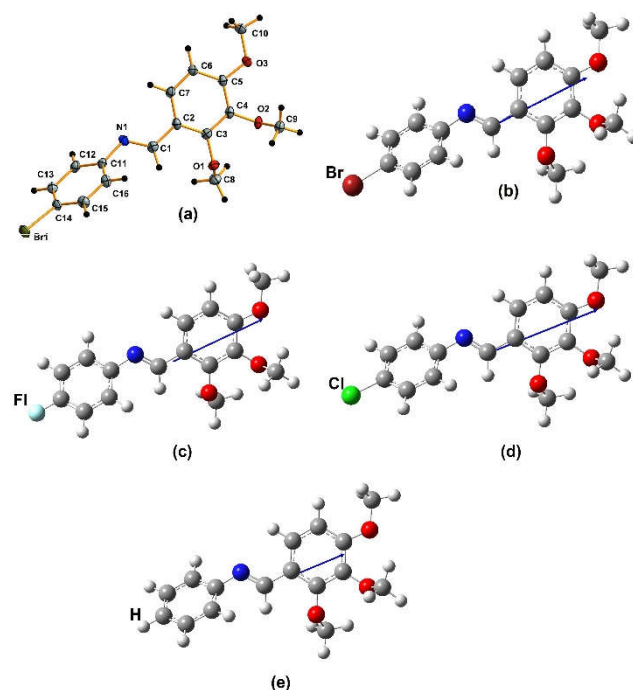


Figure 1. (a) The molecular structure of the BMBA molecule with atom-labeling scheme. Displacement ellipsoids are drawn at the 50% probability level [13]; (b) The theoretical geometric structure of BMBA; (c), (d) and (e) The theoretical geometric structure with F, Cl and H substituent, respectively

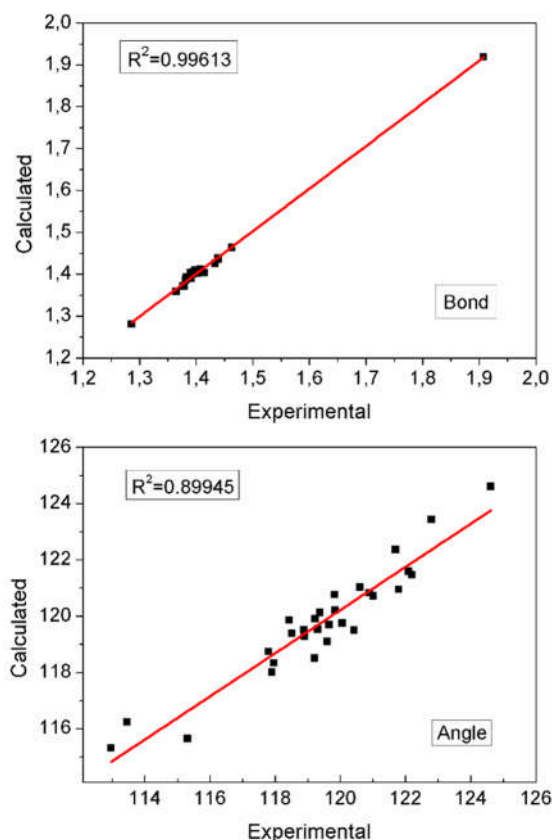


Figure 2. Comparison between calculated and experimental structural parameters of BMBA.

Optimized geometrical parameters (bond lengths, angles and dihedral angles) of the BMBA have been obtained using the B3LYP/6-311++G(d,p) method. The results can be visible in Table 1 and are compared with the experimental BMBA data [13]. The N1-C1 and N1-C11 bond lengths are found 1.281 and 1.403 Å, respectively. As found in similar experimental values, it conform to the value for a double and single bonds [13,17]. The two methoxy groups attached at C3 and C4 are twisted away from the benzene ring of C2-C7. These dihedral angles are corresponding C2C3O1C8, and C3C4O2C9 of 113.3° (103.6 (2)°), -105.21° (-88.7 (2)°) for theoretical (experimental) values, respectively. The last methoxy group attached at C5 is almost coplanar with the C2-C7 ring, as shown by the torsion angle C6C5O3C10 of -2.3° (-7.2 (3)°) for theoretical (experimental) value. When the experimental X-ray single crystal structure and optimized theoretical structure parameters of the BMBA are compared (see Fig. 2), conformational discrepancies are observed between them. To understand these discrepancies, torsion angles are compared; τ_1 (C3C2C1N1) [-159.3 (17)°] and τ_2 (C12C11N1C1) [-140.4 (18)°] for X-ray single crystal. These dihedral angles have been calculated at -178.2° and -143.7° for B3LYP, respectively. As a similar compounds containing different substituent from Group VIIA, were presented the crystal structure of C₁₆H₁₆XNO₃(X=Cl and F) [17,18].

F, Cl, Br and H atoms have the same number of electrons in the last shell. As expected, these elements have certain properties in common. In here, DFT calculations for the compounds containing the F, Cl and H in place of the Br atoms were done by the same method in order to analyze the substituent effects on the τ_1 and τ_2 torsion angles (Fig. 1). Firstly, from obtained optimized geometry we compared all structures energetically: $E_{Br} < E_{Cl} < E_F < E_H$. We see that bond length and angles agree with literature [13, 17-21]. Then, the τ_1 and τ_2 dihedral angles are calculated as -178.0° and -144.0° for Cl, -177.7° and -144.7° for F and -177.9° and -142.9 for H. These values are agree with similar molecules [19-21]. While the calculated values of the Br, Cl and H substituent torsion angles show no noticeable differences when compared to each other, the calculated F substituent torsion angle has a few difference from Br. As seen Table 1, we can say the molecular geometry of the investigated compound has been a little effected by the changes of substituent.

Table 1. Selected parameters for molecular structure of BMBA and substituent

Parameters	Exp.[13]	BMBA	^a CMBA/ ^b FMBA/ ^c MBA
Bond lengths (Å)			
Br1-C14	1.908	1.919	1.761/1.359/1.084
O1-C3	1.380	1.371	1.371/1.371/1.372
O1-C8	1.438	1.438	1.438/1.437/1.437
O2-C4	1.377	1.371	1.371/1.371/1.372
O2-C9	1.440	1.435	1.435/1.435/1.435
O3-C5	1.365	1.358	1.358/1.359/1.359
O3-C10	1.434	1.425	1.425/1.424/1.424
N1-C1	1.286	1.281	1.281/1.281/1.280
N1-C11	1.415	1.403	1.403/1.405/1.405
C1-C2	1.463	1.463	1.463/1.463/1.464
C2-C3	1.408	1.412	1.412/1.411/1.411
C2-C7	1.395	1.400	1.400/1.400/1.400
C3-C4	1.391	1.399	1.399/1.399/1.399
C4-C5	1.399	1.409	1.409/1.408/1.408
C5-C6	1.403	1.401	1.401/1.401/1.400
C6-C7	1.382	1.386	1.386/1.387/1.387
C12-C11	1.390	1.403	1.403/1.404/1.403
C16-C11	1.395	1.404	1.405/1.405/1.405
C13-C12	1.391	1.390	1.389/1.390/1.390
C14-C13	1.383	1.393	1.393/1.387/1.396
C15-C14	1.387	1.391	1.391/1.385/1.394
C16-C15	1.388	1.392	1.392/1.393/1.393
Bond angles (°)			
C8O1C3	113.46	116.23	116.21/116.17/116.12
C9O2C4	112.97	115.31	115.30/115.29/115.25
C10O3C5	117.80	118.73	118.73/118.70/118.67
C11N1C1	118.43	119.86	119.91/119.93/119.86
C2C1N1	121.70	122.36	122.32/122.28/122.25
C3C2C1	119.84	120.21	120.23/120.27/120.32
C7C2C1	122.20	121.46	121.45/121.44/121.41
C7C2C3	117.96	118.33	118.32/118.29/118.27
C2C3O1	119.60	119.09	119.11/119.13/119.18
C4C3O1	119.38	120.12	120.09/120.05/119.99
C4C3C2	121.01	120.72	120.73/120.75/120.76
C3C4O2	120.43	119.49	119.49/119.49/119.50
C5C4O2	119.83	120.76	120.75/120.75/120.74
C5C4C3	119.66	119.69	119.70/119.71/119.71
C4C5O3	115.31	115.65	115.65/115.66/115.67
C6C5O3	124.62	124.60	124.61/124.62/124.62
C6C5C4	120.06	119.75	119.74/119.72/119.71
C7C6C5	119.23	119.90	119.91/119.91/119.91
C6C7C2	122.09	121.59	121.60/121.61/121.62
C12C11 N1	117.91	118.00	117.95/117.80/117.93
C16C11N1	122.80	123.43	123.49/123.51/123.23
C16C11C12	119.21	118.50	118.49/118.63/118.79
C13C12C11	120.60	121.03	121.03/121.01/120.54
C14C13C12	118.90	119.27	119.30/118.65/120.38
C13C14Br1	119.31	119.53	119.53/118.93/120.30
C15C14Br1	118.89	119.51	119.54/118.94/120.26
C15C14C13	121.80	120.95	120.92/122.12/119.44
C16C15C14	118.52	119.38	119.41/118.77/120.48
C15C16C11	120.90	120.83	120.81/120.78/120.34
Dihedral angles (°)			
C2C3O1C8	103.6	113.3	113.1/112.9/112.6
C3C4O2C9	-88.7	-105.2	-105.1/-105.0/-104.7
C6C5O3C10	-7.2	-2.3	178.2/178.3/178.2
C2C1N1C11	-176.5	-176.8	-176.8/-176.9/-176.9

C12C11N1C1	-140.4	-143.7	-144.0/-144.7/-142.9
C3C2C1N1	-159.3	-178.2	-178.0/-177.7/-177.9

^aCMBA: 4-Chloro-*N*-(2,3,4-trimethoxybenzylidene)aniline

^bFMBA: 4-Fluoro-*N*-(2,3,4-trimethoxybenzylidene)aniline

^cMBA: *N*-(2,3,4-trimethoxybenzylidene)aniline

3.2. Conformational analysis

For defining the favored position of low energy structures computations were performed using B3LYP/6-311++G(d,p) as a function of the selected degrees of torsional freedom $\tau(\text{C3C2C1N1})$, which was varied from -180° to $+180^\circ$ in steps of 20° . The respective values of the selected degrees of torsional freedom, $\tau(\text{C3C2C1N1})$, is -159.3° in X-ray single crystal structure [13], but it is -178.2° in DFT optimized geometry. In Fig. 3, we have shown the molecular energy profiles (Hartree) with respect to rotations about the selected torsion angle (degree). It is seen from Fig. 3 that the low energy domains is located at -178.2° , optimized geometry. Also, it has two saddle point at -80° and 80° . Besides second favorable conformer is calculated at -40° torsional value as metastable structure.

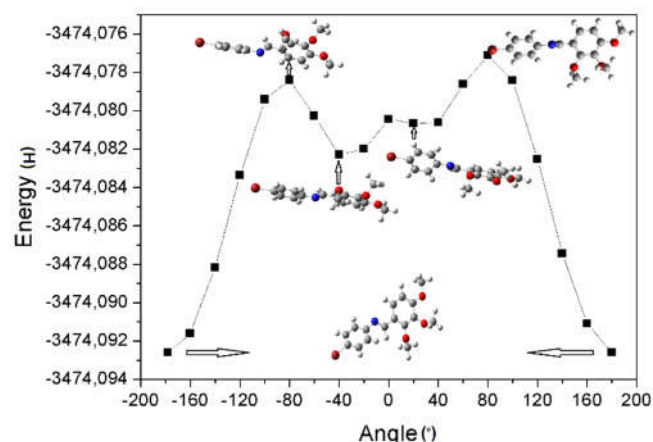


Figure 3. Potential energy surface scan using B3LYP/6-311++G(d,p) method for $\tau(\text{C3C2C1N1})$ dihedral angle of the title compound

3.3. Vibrational spectra

The BMBA molecule consists of 37 atoms, which undergo 105 normal modes of vibrations. The harmonic frequencies along with intensities were computed with the help of Gauss View program and were illustrated in Table 2. C-H aromatic and aliphatic experimental frequencies appeared between 2911 and 2998 cm^{-1} [13]. The characteristic region of vibrational stretchings are appeared between 3000 and 3100 cm^{-1} in general.

In this study, C-H (aromatic) frequencies are estimated at $3051\text{--}3083\text{ cm}^{-1}$. The -CH=N- (aliphatic) in-plane bending vibration is observed at 2942 cm^{-1} . This vibration is agreement with experimental over the range. The bending vibrations of C-H in plane/out of plane are located at $1000\text{--}1300/800\text{--}950\text{ cm}^{-1}$, respectively [22-25]. In here the C-H in plane (out of plane) bending vibrations are found in the range $1075\text{--}1463\text{ cm}^{-1}$ ($788\text{--}982\text{ cm}^{-1}$). Three methoxyl groups connected with the phenyl group, the C-O stretching vibrations associated with the ring are calculated at 1199 and 1260 cm^{-1} and below this value in the mixed modes. This mode was found at 1209 cm^{-1} in FT-IR spectrum by Joshi *et al.* [26]. The C-O in-plane bending is calculated at 752 cm^{-1} in the highly mixed modes.

In [13], C=C aromatic frequency is given at $1413\text{--}1594\text{ cm}^{-1}$. The vibrations of C=C and C-C stretchings are found in the region of $1390\text{--}1620\text{ cm}^{-1}$ [27] and $1280\text{--}1625\text{ cm}^{-1}$ [28]. In this study, C=C and C-C stretching vibrations are very prominent at $1242\text{--}1564\text{ cm}^{-1}$ and $1019\text{--}1463\text{ cm}^{-1}$ region. The vibration modes containing the ring CCC were also observed at $674\text{--}1037\text{ cm}^{-1}$ region in the FT-IR spectra. The task identification of C=N, C-N vibrations are very difficult because of the possibility mixing of several bands in these regions. In the literature, the C-N vibrational stretchings are found in between 1266 and 1382 cm^{-1} [29], 1120 and 1150 cm^{-1} [30], and 1200 and 1300 cm^{-1} [31]. In this work, these modes are labelled at 846 and 1186 cm^{-1} for BMBA. Schiff-bases proton transfer can be identified by using the characteristic region of $1700\text{--}1500\text{ cm}^{-1}$. C=N (azomethine) stretching vibration was appeared at 1606 and 1534 cm^{-1} . Hence it has been observed at 1615 cm^{-1} for experimental value [13]. In this study, the in-plane and out-of-plane bending vibrations of carbon-nitrogen group are assigned which are also supported by the literature [32]. The C-Br vibrations are often found over the $480\text{--}1290\text{ cm}^{-1}$ range since its vibration is easily affected by the adjacent atoms or groups [33,34]. In here, the medium bands at 1037 cm^{-1} is assigned to C-Br stretching vibration coupled with ring deformation. Additionally, for the compounds containing the Cl, F and H in place of the Br atoms frequencies were calculated and added in Table 2. C-Cl vibrations are in the region $480\text{--}1129\text{ cm}^{-1}$ for simple chlorine compounds [35,36]. The C-Cl stretching vibrations was observed at 1056 and 1096 cm^{-1} in FT-IR spectrum [37]. In this study, it

was observed at 1054 cm⁻¹. Normally, the C-F stretching vibrations appear in the region 1000-1300 cm⁻¹ for several fluoro-benzenes as very strong in the IR spectra [38]. As this region, the corresponding C-F stretching vibration is observed at 1171 and 1193 cm⁻¹. The other vibrational frequencies can be seen in Table 2. These BMBA and substituent (Cl/F/H) vibrations are also in agreement with each other.

Table 2. Vibrational wavenumbers of BMBA and substituents, in cm⁻¹, and assignments

927	927/927/926	δ(C-H)R2+v(CH ₃ -O-C)sM
847	848/853/841	v(C-N)s+β(CCC)
809	811/820/810	ω(C-H)R2
788	788/788/788	ω(C-H)R1
752	754/726/757	β(CCC)+β(COC)
690	700/697/678	τ(CCC)R2
675	680/667/671	β(CCC)R
646	647/647/647	τ(CCC)R1
619	621/624/607	β(CCC)R2
577	582/584/585	τ(CCC)R1+β(CCC)R2

^a v, stretching; α, scissoring; ω, wagging; γ, rocking; δ, twisting; β, bending(in plane); τ, torsion(out of plane); s, symmetric; as, asymmetric. Abbreviations: M1, methy(C13); M2, methy(C14); M3, methy(C15); M, M1M2M3; R1, C2-C7; R2, C11-C16 ring; R, R1 and R2.

BMBA	Theoretical		Assignments ^a
	CMBA/FMBA/MBA		
3083	3083/3082/3082		v(C-H)s R1
3071	3070/3071/3064		v(C-H)s R2
3067	3067/3067/3066		v(C-H)as R1
3058	3058/3060/3058		v(C-H)as R2
3051	3051/3054/3052		v(C-H)as R2
3013	3013/3013/3012		v(C-H ₃)as M3
3011	3011/3010/3009		v(C-H ₃)as M1
3005	3004/3004/3004		v(C-H ₃)as M2
2976	2976/2975/2974		v(C-H ₃)as M1
2967	2967/2967/2966		v(C-H ₃)as M2
2952	2952/2951/2951		v(C-H ₃)as M3
2942	2941/2940/2941		v(-CH=N-)s
2900	2900/2899/2899		v(C-H ₃)s M2
2898	2897/2897/2897		v(C-H ₃)s M1
2892	2892/2892/2891		v(C-H ₃)s M3
1606	1607/1608/1609		v(C=N)s
1564	1566/1573/1570		v(C=C)s+β(CCC)R
1547	1550/1556/1554		v(C=C)s+v(C=N)s
1463	1464/1469/1464		γ(C-H)R+v(C-O)+s v(C-C)
1449	1450/1461/1455		γ(C-H)R1+α (C-H ₃)M
1444	1444/1450/1450		α(C-H ₃)M1
1444	1444/1444/1444		α(C-H ₃)M2,M3
1432	1433/1433/1433		α(C-H ₃)M3
1430	1430/1430/1430		α(C-H ₃)M2
1424	1424/1424/1424		α(C-H ₃)M1
1411	1410/1410/1409		v(C=C)s+ω(C-H ₃)M
1384	1384/1385/1384		ω(C-H ₃)M+γ(C-H)
1334	1334/1334/1334		γ(C-H)+ v(C-C)s
1273	1273/1274/1273		v(C=C)s+γ(C-H)
1260	1260/1260/1260		v(C=C)R1+γ(C-H)+v(C-O)
1252	1253/1258/1259		v(C=C)R2+γ(C-H)+v(C-O)
1242	1241/1240/1239		v(C=C)R1+γ(C-H)+v(C-C)
1199	1198/1199/1198		ω(C-H ₃)M+v(C-O)s
1186	1186/1193/1185		v(C-N)s+v(C-F)
1174	1174/1171/1173		α(C-H)R1+v(C-N)+v(C-F)
1152	1152/1152/1152		ω(C-H ₃)M1,M2
1144	1142/1141/1143		α(C-H)R2
1141	1141/1122/1140		α(C-H)R1
1121	1121/1121/1121		δ(C-H ₃)M
1075	1075/1075/1075		v(C-O)s+α(C-H)R1
1037	1054/ - / -		v(CBr(Cl))as+β(CCC)
1019	1019/1019/1019		v(CH ₃ -O)sM+v(C-C)s
992	992/992/993		v(CH ₃ -O)sM+β(CCC)
982	984/985/979		δ(C-H)+β(CCC)
937	936/932/940		δ(C-H)R2
931	931/930/931		δ(C-H)R1

3.4. Frontier molecular orbitals

According to the frontier orbital theory the reactivity of reactants is largely dependent on the energies of the frontier molecular orbitals (FMO) [39]. The investigation on the FMO energy levels of BMBA give us that the corresponding electronic transfers happened between the HOMO -1 and LUMO+1. The predicted frontier molecular orbital for BMBA is depicted in Fig. 4. Both the HOMO and the LUMO are mostly the π-antibonding type orbitals. The value of the energy separation between the HOMO and LUMO is 4.079 eV. From the Fig. 4, electrons in the HOMO-1, HOMO and LUMO are localized all over the molecule, whereas electrons in the LUMO+1 are mainly found on the C11-C16 benzene ring. It is clearly visible that the charge density in the isolated molecule is shifting from one portion of the molecule to the other. In case of LUMO the charge is mainly accumulated from the phenyl ring. In LUMO the charge is acquired by the same parts significantly.

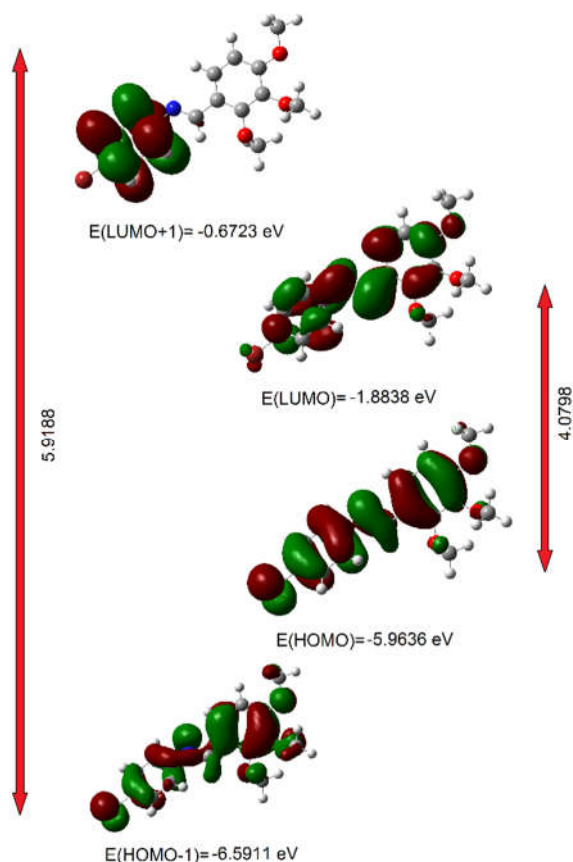


Figure 4. Molecular orbital surfaces and energy levels given in parantheses for the HOMO-1, HOMO, LUMO and LUMO+1 of BMBA

We have also calculated global hardness and global softness to investigate chemical reactivity and stability of BMBA. Also, considering the chemical hardness, large HOMO-LUMO gap (ΔE_{H-L}) means a hard molecule and small ΔE_{H-L} means a soft molecule. The global hardness is $\eta = (E_{LUMO} - E_{HOMO})/2$ and softness is $S = 1/2\eta$ [12], in which E_{LUMO} and E_{HOMO} are defined as LUMO and HOMO energies, respectively. η , S , E_{LUMO} , E_{HOMO} and ΔE_{H-L} for BMBA are calculated as 2.040 eV, 0.245 eV⁻¹, -1.883 eV, -5.963 eV and 4.079 eV, respectively.

3.5. Molecular electrostatic potential

Molecular electrostatic potential (MEP) regions having partially negative charge and defined as red-electron rich were connected to electrophilic reactivity. Moreover, MEP regions having partially positive charge and defined as the blue-electron deficient were connected to nucleophilic reactivity and it can be seen in Fig. 5. The total electron density extreme limits are -0.035 to +0.035 a.u.

The MEP clearly indicates regions having the negative potential were observed around the O1,

O2, O3, N and Br atoms. These negative values of $V(r)$ are -0.028, -0.035, -0.033 and -0.023 a.u. for O1, O2-O3, N and Br atoms, respectively. From these values, we can say that oxygen atoms of the BMBA molecule would be preferred sites for an electrophilic attack. Moreover, in MEP, positive regions are located on the C-H bonds between value of +0.028 with +0.015 a.u. Thus, these regions are indicated as favored sites for nucleophilic interaction where chemical bonding and molecule interact with one another can take place [22]. The MEP mapping is also very useful in understanding hydrogen bonding interactions [40].

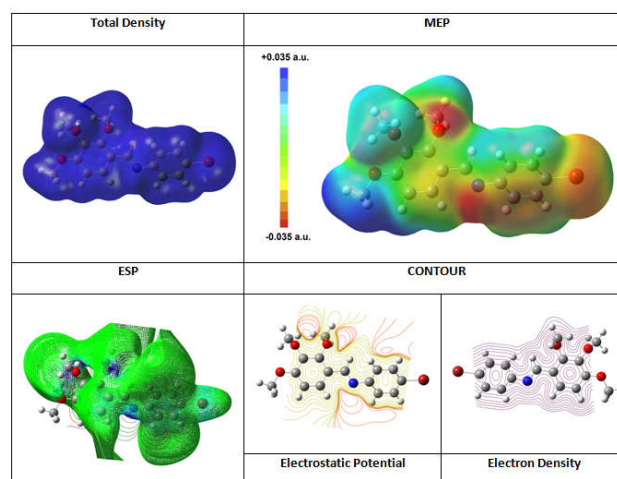


Figure 5. The total electron density mapped with electrostatic potential surface of BMBA

3.6. Nonlinear optics

NLO materials are utilised in applications including telecommunications, signal processing, optical interconnections, etc. The nonlinear optical property is associated with molecular nonlinear polarization [41].

The non-linear polarization (p) for a molecule, can be calculated as follows

$$p = \mu_0 + \alpha_{ij} E_j + \beta_{ijk} E_j E_k + \dots \quad (3.6.1)$$

where μ_0 , α_{ij} and β_{ijk} are the permanent dipole moment, the linear polarizability and the first hyperpolarizability tensor components, respectively. Using the x, y, z components, μ , α and β can be calculated as:

$$\mu = \sqrt{\mu_x^2 + \mu_y^2 + \mu_z^2} \quad (3.6.2)$$

$$\alpha = \frac{\alpha_{xx} + \alpha_{yy} + \alpha_{zz}}{3} \quad (3.6.3)$$

$$\beta = \sqrt{(\beta_{xxx} + \beta_{xyy} + \beta_{xzz})^2 + (\beta_{yyy} + \beta_{yzz} + \beta_{yxx})^2 + (\beta_{zzz} + \beta_{zxx} + \beta_{zyy})^2} \quad (3.6.4)$$

The electronic dipole moment μ_i ($i=x,y,z$), polarizability α_{ij} and the first hyperpolarizability β_{ijk} of BMBA obtained by DFT-B3LYP method and the 6-311++G(d,p) basis set are reported in Table 3. μ is calculated as 5.26 D. In here, the highest value for μ is found μ_x as 5.23 D for the molecule. The polarizability α , is calculated 39.73 Å³. The calculated value of β is 6.47×10^{-30} cm⁵/esu, which is grater than that of urea (β of urea is 0.77×10^{-30} cm⁵/esu obtained by B3LYP/6-311++G(d,p)). The first order hyperpolarizability of BMBA is nearly 8.40 times of urea. We conclude that BMBA is an attractive object for future studies of NLO material.

Table 3. The calculated μ , α and β components

Paramet.	Compounds			
	BMBA	CMBA	FMBA	MBA ^c
μ_x	5.23	5.14	4.76	2.90
μ_y	-0.53	-0.60	-0.64	-0.32
μ_z	-0.11	-0.09	-0.08	-0.10
μ (Debye)	5.26	5.18	4.80	2.92
α_{xx}	438.59	417.94	374.08	370.74
α_{xy}	-11.11	-11.48	-8.22	-9.70
α_{yy}	218.27	213.67	207.54	207.92
α_{xz}	-6.75	-5.75	-5.57	-4.61
α_{yz}	-10.48	-11.02	-11.28	-11.34
α_{zz}	148.30	143.23	136.82	138.95
α (Å ³)	39.73	38.23	35.45	35.41
β_{xxx}	-721.71	-628.32	-509.76	-1251.24
β_{xxy}	309.07	292.60	297.83	377.32
β_{xyy}	16.39	26.28	8.37	-30.62
β_{yyy}	-162.52	-174.48	-172.69	-159.47
β_{xxz}	97.46	69.33	70.02	20.18
β_{xyz}	-17.30	-3.41	15.53	-21.67
β_{yyz}	7.76	1.60	4.74	14.20
β_{zzz}	-27.24	-6.45	-2.37	-47.38
β_{yzz}	-31.11	-40.75	-35.90	-30.87
β_{zzz}	3.03	-4.04	5.79	0.78
β (cm ⁵ /esu)	6.47×10^{-30}	5.33×10^{-30}	4.47×10^{-30}	11.60×10^{-30}

For the investigation of the substituent effects on the NLO properties, μ , α and β were calculated for the molecules having the Cl, F and H instead of Br atom of BMBA (Table 3). From Table 3, one can easily assume that the calculated values of μ were a little affected by the substituents. These values of μ and α for the BMBA compound are bigger than those of substituent. Besides, the calculated values of β have minor differences from each other except for H substituent compound.

4. CONCLUSIONS

The equilibrium geometries, vibrational frequencies and vibrational assignments of the

BMBA molecule were determined and analyzed. These vibrational assignments along with the electronic transitions are important to understand the molecular. Optimized geometric structure and vibrational assignments show a good agreement with results obtained from experiments.

The mapping electron density give information about the shape, size and charge density distribution. Molecular electrostatic potential of BMBA indicates that the positive potential sites are around the hydrogen atoms while the negative potential sites are on oxygen atoms and phenyl rings. HOMO-LUMO made very clearly the involvement of charge transfer between the donor and acceptor groups. The NLO is identified as a featured attribute of BMBA which was inspected and authenticated via computed polarizability and hyperpolarizability. The calculated hyperpolarizability of BMBA is much higher than the standard NLO material urea.

ACKNOWLEDGMENTS

This research was assisted by The Amasya University Research Centre under the Projects Number of FMB-BAP 15-092.

REFERENCES

- [1] J. H. Choi, H. Y. Lee, A. D. Towns, "Dyeing properties of novel azo disperse dyes derived from phthalimide and color fastness on poly (lactic acid) fiber," *Fiber Polym.* Vol. 11, no. 2, pp. 199-204, 2010.
- [2] E. N. Shepelenko, A. V. Tsukanov, Y. V. Revinskii, A. D. Dubonosov, V. A. Bren, V. I. Minkin, "Benzoid-quinoid tautomerism of schiff bases and their structural analogs: LIII. Schiff bases derived from 5-hydroxy- and 5-hydroxy-6-nitro-2, 3-diphenyl-1-benzofuran-4-carbaldehydes," *Russ. J. Org. Chem.* vol. 43, no. 4, pp. 559-562, 2007.
- [3] E. Hadjoudis, A. Ronroyianni, K. Ambroziak, T. Dziembowska, I. M. Mavridis, "Photochromism and thermochromism of solid trans-N, N'-bis-(salicylidene)-1, 2-cyclohexanediamines and trans-N, N'-bis-(2-hydroxy-naphylidene)-1, 2-cyclohexanediamine," *J. Photochem. Photobiol. A* vol. 162, no. 2, pp. 521-530, 2004.

- [4] C. M. da Silva, D. L. da Silva, L. V. Modolo, R. B. Alves, M. de Resende, C. V. B. Martins, A. de Fatima, "Schiff bases: A short review of their antimicrobial activities," *J. Adv. Res.* Vol. 2, no. 1, pp. 1-8, 2011.
- [5] J. H. Choi, J. Y. Choi, H. Y. Lee, A. D. Towns, C. Yoon, "Novel azo dyes derived from phthalimide. Part 2: Dyeing properties and colour fastness on polyester fibres," *Coloration Technology*, vol. 124, no. 6, pp. 364-369, 2008.
- [6] R. Pignatello, A. Panico, P. Mazzane, M. R. Pinizzotto, A. Garozzo, P. M. Fumeri, "Schiff bases of N-hydroxy-N'-aminoguanidines as antiviral, antibacterial and anticancer agents," *European journal of medicinal chemistry*," vol. 29, no. 10, pp. 781-785, 1974.
- [7] D. R. Williams, "Metals, ligands, and cancer," *Chemical reviews*, vol. 72, no.3, pp. 203-213, 1972.
- [8] L. Sundararaman, R. Kandasamy, H. Stoeckli-Evans, V. Gopalsamy, "[4-Chlorophenyl] iminomethyl phenol," *Acta Crystallographica Section E: Structure Reports Online*, vol. 63, no. 12, pp. 4805-4805, 2007.
- [9] K. Srinivasan, R. Biravaganesh, R. Gandhimathi, P. Ramasamy, "Growth and characterization of NMBA (4-nitro-4'-methyl benzylidene aniline) single crystals," *Journal of crystal growth*, vol. 236, no. 1-3, pp. 381-392, 2002.
- [10] M. Aslantas, E. Kendi, N. Demir, A. E. Sabik, M. Tumer, M. Kertmen, "Synthesis, spectroscopic, structural characterization, electrochemical and antimicrobial activity studies of the Schiff base ligand and its transition metal complexes," *Spectrochimica Acta Part A: Molecular and Biomolecular Spectroscopy*, vol. 74, no. 3, pp. 617-624, 2009.
- [11] Y. Sun, Y. Wang, Z. Liu, C. Huang, C. Yu, "Structural, proton-transfer, thermodynamic and nonlinear optical studies of (E)-2-((2-hydroxyphenyl) iminiomethyl) phenolate," *Spectrochimica Acta Part A: Molecular and Biomolecular Spectroscopy*, vol. 96, pp. 42-50, 2012.
- [12] A. Subashini, R. Kumaravel, S. Leela, H. S. Evans, D. Sastikumar, K. Ramamurthi, "Synthesis, growth and characterization of 4-bromo-4' chloro benzylidene aniline—A third order non linear optical material," *Spectrochimica Acta Part A: Molecular and Biomolecular Spectroscopy*, vol. 78, no. 3, pp. 935-941, 2011.
- [13] K. Fejfarová, A. D. Khalaji, M. Dušek, "(E)-4-Bromo-N-(2, 3, 4-trimethoxybenzylidene) aniline," *Acta Crystallographica Section E: Structure Reports Online*, vol. 66, no. 8, pp. 2062-2062, 2010.
- [14] M. J. Frisch et al, Gaussian 09, Revision C. 01, Gaussian Inc., Wallingford CT, 2009.
- [15] R. Dennington, T. Keith, J. Millam, Semichem Inc, Shawnee Mission KS, GaussView, Version 5 (2009).
- [16] H. Tanak, A. A. Agar, O. Büyükgüngör, "Combined experimental and DFT computational studies on (E)-1-(5-nitrothiophen-2-yl)-N-[4-(trifluoromethyl) phenyl] methanimine," *Journal of Molecular Structure*, vol. 1048, pp. 41-50, 2013.
- [17] R. K. Balachandar, S. Kalainathan, S. M. Eappen, J. Podder, "4-Fluoro-N-[(E)-3, 4, 5-trimethoxybenzylidene] aniline," *Acta Crystallographica Section E: Structure Reports Online*, vol. 69, no. 8, pp. 1234-1234, 2013.
- [18] A. Dehno Khalaji, J. Asghari, K. Fejfarová, M. Dušek, "4-Chloro-N-(3, 4, 5-trimethoxybenzylidene) aniline," *Acta Crystallographica Section E: Structure Reports Online*, vol. 65, no. 2, pp. o253-o253, 2009.
- [19] D. Mahadevan, S. Periandy, M. Karabacak, S. Ramalingam, "FT-IR and FT-Raman, UV spectroscopic investigation of 1-bromo-3-fluorobenzene using DFT (B3LYP, B3PW91 and MPW91PW91) calculations," *Spectrochimica Acta Part A: Molecular and Biomolecular Spectroscopy*, vol. 82, no. 1, pp. 481-492, 2011.
- [20] S. Ramalingam, S. Periandy, B. Elanchezian, S. Mohan, "FT-IR and FT-Raman spectra and vibrational investigation of 4-chloro-2-fluoro toluene using ab initio HF and DFT (B3LYP/B3PW91) calculations," *Spectrochimica Acta Part A: Molecular and Biomolecular Spectroscopy*, vol. 78, no. 1, pp. 429-436, 2011.

- [21] H. Tanak, "Crystal structure, spectroscopy, and quantum chemical studies of (E)-2-[(2-Chlorophenyl) iminomethyl]-4-trifluoromethoxyphenol," *The Journal of Physical Chemistry A*, vol. 115, no. 47, pp. 13865-13876, 2011.
- [22] V. Krishnakumar, N. Prabavathi, "Simulation of IR and Raman spectral based on scaled DFT force fields: a case study of 2-amino 4-hydroxy 6-trifluoromethylpyrimidine, with emphasis on band assignment," *Spectrochimica Acta Part A: Molecular and Biomolecular Spectroscopy*, vol. 71, no. 2, pp. 449-457, 2008.
- [23] A. Altun, K. Gölcük, M. Kumru, "Structure and vibrational spectra of p-methylaniline: Hartree-Fock, MP2 and density functional theory studies," *Journal of Molecular Structure: THEOCHEM*, vol. 637, no. 1-3, pp. 155-169, 2003.
- [24] S. J. Singh, S. M. Pandey, "Vibrational-spectra of some fluoroaminotoluenes," *Indian Journal of Pure and Applied Physics*, vol. 12, no.4, pp. 300-302, 1974.
- [25] S. Muthu, E. Isac Paulraj, "Spectroscopic and molecular structure (monomeric and dimeric structure) investigation of 2-[(2-hydroxyphenyl) carbonyloxy] benzoic acid by DFT method: A combined experimental and theoretical study," *Journal of Molecular Structure*, vol. 1038, pp. 145-162, 2013.
- [26] B. D. Joshi, P. N. Chaudhary, "Molecular structure, MESP, homo-lumo and vibrational analysis of β -asarone using density functional theory," *Kathmandu Univ J Sci Eng Tech*, vol. 9, pp. 1-14, 2013.
- [27] M. Arivazhagan, V. Krishnakumar, R. John Xavier, G. Ilango, V. Balachandran, "FTIR, FT-Raman, scaled quantum chemical studies of the structure and vibrational spectra of 1, 5-dinitronaphthalene," *Spectrochimica Acta Part A: Molecular and Biomolecular Spectroscopy*, vol. 72, no. 5, pp. 941-946, 2009.
- [28] G. Varsanyi, *Vibrational Spectra of Benzene Derivatives*, Academic Press, New York, 1969.
- [29] U. Karunanithi, S. Arulmozhi, M. Dinesh Raja and J. Madhavan, "Growth and Characterization of Pure and Doped L-Phenylalanine Maleate Single Crystals," *Int. J. Eng. Res. Dev.*, vol. 3, no. 1, pp.51-55, 2012.
- [30] M. Irani, R. Ranjbar-Karimi, H. Izadi, "Synthesis and Pesticide Activity of some New Arylic and Pyridylic Oxime Ether Derivatives of Ionone," *Organic Chemistry Research*, vol. 2, no. 2, pp. 192-196, 2016.
- [31] J.B. Lambert, H.F. Shurvell, D.A. Lightner, R.G. Cooks, *Org. Struct. Spectrosc.*, Simon & Schuster/A Viacom Company, New Jersey, 1998.
- [32] B. Smith, *Infrared Spectra Interpretation. A Systematic Approach*, CRC Press, Washington, DC, 1999.
- [33] E. F. Mooney, "The infrared spectra of chloro-and bromobenzene derivatives—I: Anisoles and phenetoles," *Spectrochimica Acta*, vol. 19, no. 6, pp. 877-887, 1963.
- [34] E. F. Mooney, "The infra-red spectra of chloro-and bromobenzene derivatives—II. Nitrobenzenes," *Spectrochimica Acta*, vol. 20, no. 6, pp. 1021-1032, 1964.
- [35] K. Rastogi, M. A. Palafox, R. P. Tanwar, L. Mittal, "3, 5-Difluorobenzonitrile: ab initio calculations, FTIR and Raman spectra," *Spectrochimica Acta Part A: Molecular and Biomolecular Spectroscopy*, vol. 58, no. 9, pp. 1989-1997, 2002.
- [36] H. Tanak, M. Toy, "Molecular structure, spectroscopic and quantum chemical studies on 2'-chloro-4-dimethylamino azobenzene," *Journal of Molecular Structure*, vol. 1068, pp. 189-197, 2014.
- [37] M. Evecen, G. Duru, H. Tanak, A.A. Ağar, "Synthesis, crystal structure, spectral analysis and DFT computational studies on a novel isoindoline derivative," *Journal of Molecular Structure*, vol. 1118, pp. 1-9, 2016.
- [38] M. P. Kumpawat, A. Ojha, N. D. Patel, "Vibrational-spectra and normal coordinate analysis of some substituted anilines," *Canadian Journal of Spectroscopy*, vol. 25, no. 1, pp. 1-14, 1980.
- [39] I. Fleming, "Frontier Orbitals and Organic Chemical Reactions," Wiley, London, 1976.
- [40] N. Okulik, A. H. Jubert, "Theoretical analysis of the reactive sites of non-steroidal anti-inflammatory drugs," *Internet*

Electronic Journal of Molecular Design,
vol. 4, no. 1, pp. 17-30, 2005.

studies of 4-(1, 3-dioxoisindolin-2-yl)
antipyrine," *Journal of Molecular Structure*,
vol. 1030, pp. 113–124, 2012.

- [41] Z. Yu, G. Sun, Z. Liu, C. Yu, C. Huang, Y. Sun, "Synthesis, crystal structure, vibrational spectral and density functional